Australian Government
Department of Defence
Defence Science and
Technology Organisation

Initial Trial using Embedded Fibre Bragg Gratings for Distributed Strain Monitoring in a Shape Adaptive Composite Foil

Claire Davis, Patrick Norman, James Kopczyk and David Rowlands

Air Vehicles Division
Defence Science and Technology Organisation

DSTO-TN-1070

ABSTRACT

This technical note reports on the embedment and testing of a series of distributed optical fibre sensors embedded just beneath the top and bottom surfaces of a shape adapative composite foil. The sensors were monitored during the resin infusion and curing stages of the composite foil fabrication process. The cured foil was tested in a variable pressure water tunnel at different flow rates, angles of attack and tunnel pressures to characterise the distributed strain response of the foil to these parameters.

RELEASE LIMITATION

Approved for public release

Published by

Air Vehicles Division
DSTO Defence Science and Technology Organisation
506 Lorimer St
Fishermans Bend, Victoria 3207 Australia

Telephone: (03) 9626 7000
Fax: (03) 9626 7999

AR-015-236
February 2012

APPROVED FOR PUBLIC RELEASE

Initial Trial using Embedded Fibre Bragg Gratings for Distributed Strain Monitoring in a Shape Adaptive Composite Foil

Executive Summary

The work described in this technical note supports the smart propeller activity in the Signatures, Materials and Energy Corporate Enabling Research Program (SME-CERP). The aim of the smart propeller activity is to develop and evaluate the capability to perform in-situ monitoring, and non-destructive evaluation, of the structural fatigue and hydrodynamic performance of composite materials.

In order to avoid the significant practical challenges associated with experimental measurements of deflection and strain on a full-scale rotating propeller, a composite foil specimen amenable to a laboratory investigation was designed to experience similar loading and deflections to a full-scale propeller blade.

The shape adapative composite foil specimen was fabricated with a series of distributed optical fibre sensors embedded just beneath the top and bottom surfaces. The sensors were monitored during the resin infusion and curing stages of the fabrication process. The cured foil was tested in a variable pressure water tunnel at the Australian Maritime Collage (AMC) Cavitation Research Laboratory (CRL) at different flow rates, angles of attack and tunnel pressures to characterise the distributed strain response of the foil to these parameters.

This data will be used to validate the analytical techniques and manufacturing methods used in creating the foil.

This page is intentionally blank

Contents

This page is intentionally blank

1. Background

Bragg gratings in optical fibres offer the potential to overcome some of the engineering challenges associated with using high density distributed strain sensing to achieve in-situ measurement of the deflection shape of composite structures. Optical fibre sensors are immune to electromagnetic interference, inherently corrosion-resistant and their size and weight allow them to be incorporated into composite structures with minimal intrusion. The number of sensors that can be written on a single fibre is limited only by the physical length of the gratings (usually a few mm) and the bandwidth of the source available for interrogation. Although commercially available fibre Bragg grating (FBG) sensors have emerged in the marketplace over the past decade, generally these sensors are packaged for surface-mounting to achieve a single point measurement of strain and/or temperature.

This report documents the results from a preliminary trial investigating the feasibility of using embedded FBG arrays in a shape adaptive composite foil to characterise the distributed strain response of the foil in a variable pressure water tunnel at different flow rates, angles of attack (AoA) and tunnel pressures. The response from the FBG sensors was also monitored during fabrication of the foil during the resin infusion and curing stages of the process.

1.1 Principle of Operation of Fibre Bragg Gratings

A fibre Bragg grating is a periodic modulation in the refractive index of the core of an optical fibre. The periodic modulation is achieved by exposing the fibre (side-on) to two interfering UV laser beams. The refractive index is altered via modification of the oxygen vacancy-defect absorption band by the UV light.

Fibre Bragg gratings typically reflect light over a narrow wavelength range and transmit all other wavelengths. They are based on the principle of Bragg reflection where if light propagates through periodically alternating regions of higher and lower refractive index, it is partially reflected at each interface between those regions. If the spacing between these regions is such that all the partial reflections add up in phase and the roundtrip of the light between two reflections is an integral number of wavelengths then the Bragg condition is satisfied and the total reflection can grow to nearly 100% as shown in Figure 1.

The reflected wavelength, known as the Bragg wavelength, is related to the grating period by the following equation:

$$\lambda_{Bragg} = 2n\Lambda$$

where n is the average refractive index of the fibre and Λ is the period of the grating. Changes in axial strain and/or temperature along the fibre will alter the period of the index modulation and result in a shift of the reflected Bragg wavelength. Assuming a constant temperature, this shift in wavelength is linearly proportional to the axial strain experienced by the fibre. The gauge factor for FBGs is approximately 1.2 pm per μstrain and 10 pm per degree Celsius for standard optical fibre.

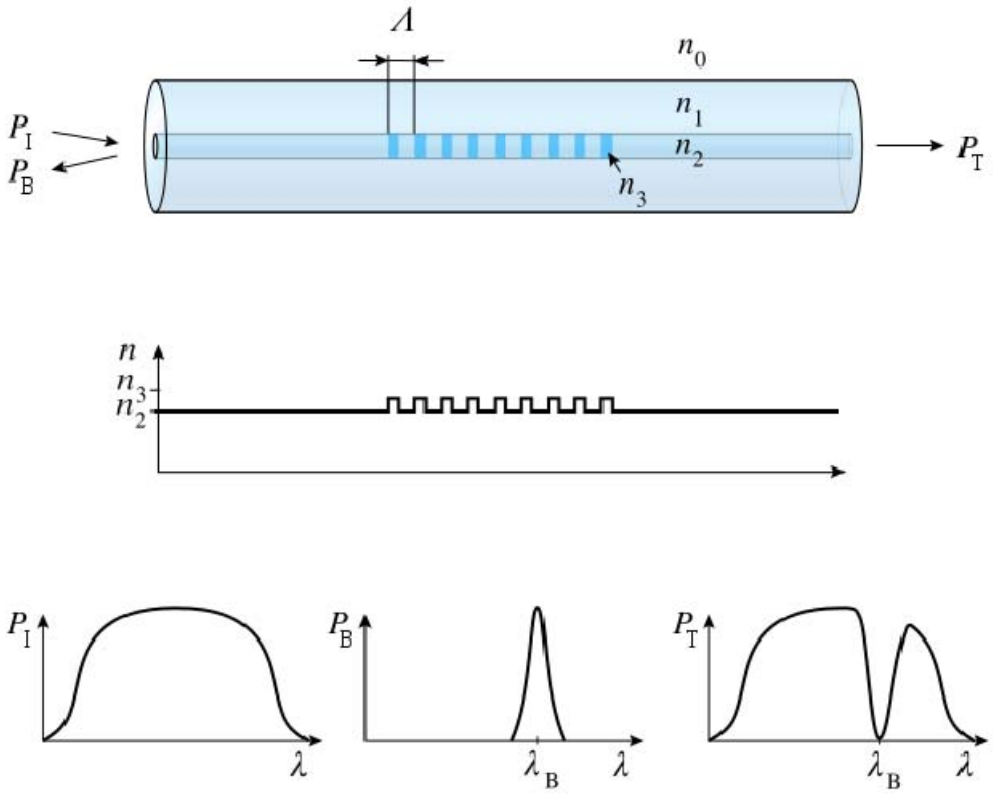

Figure 1: Principle of operation of a Bragg fibre grating

2. Introduction

The optical fibres were included during the lay-up of the composite foil prior to resin infusion as shown in Figure 2.

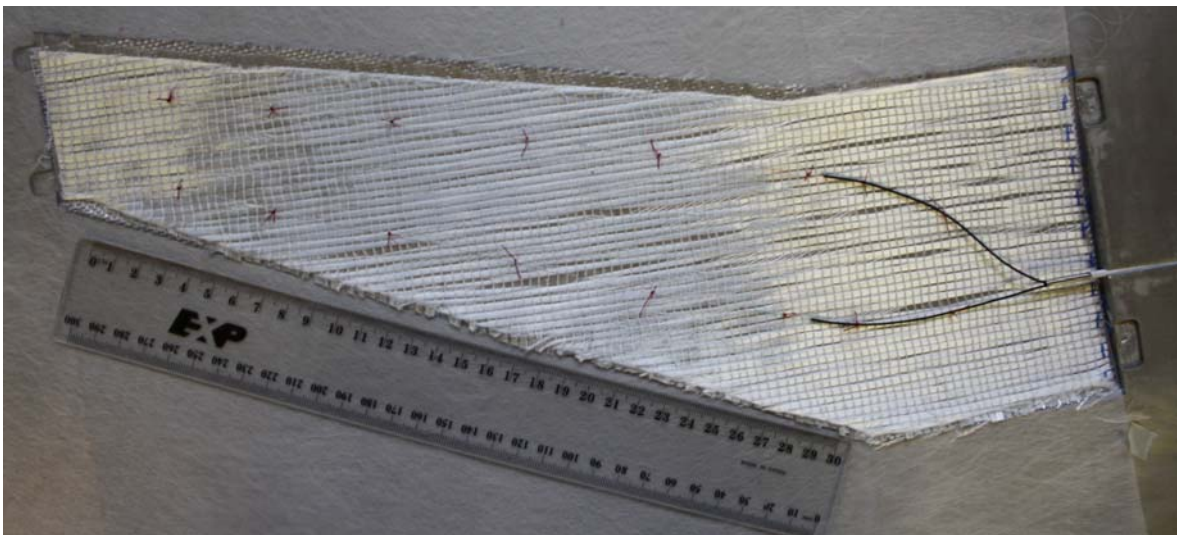

Figure 2: Optical fibres shown stitched to the final woven glass ply prior to resin infusion

Two optical fibres containing FBG arrays were stitched into the final woven glass ply on the top and bottom surfaces of the foil respectively before inclusion in a closed Aluminium mould. The stitches were made between the optical fibre and the weave fibre on the E-glass fabric approximately 20 mm on either side of each FBG so as to minimise any transverse strain on the fibre in the active sensing area as shown in Figure 3.

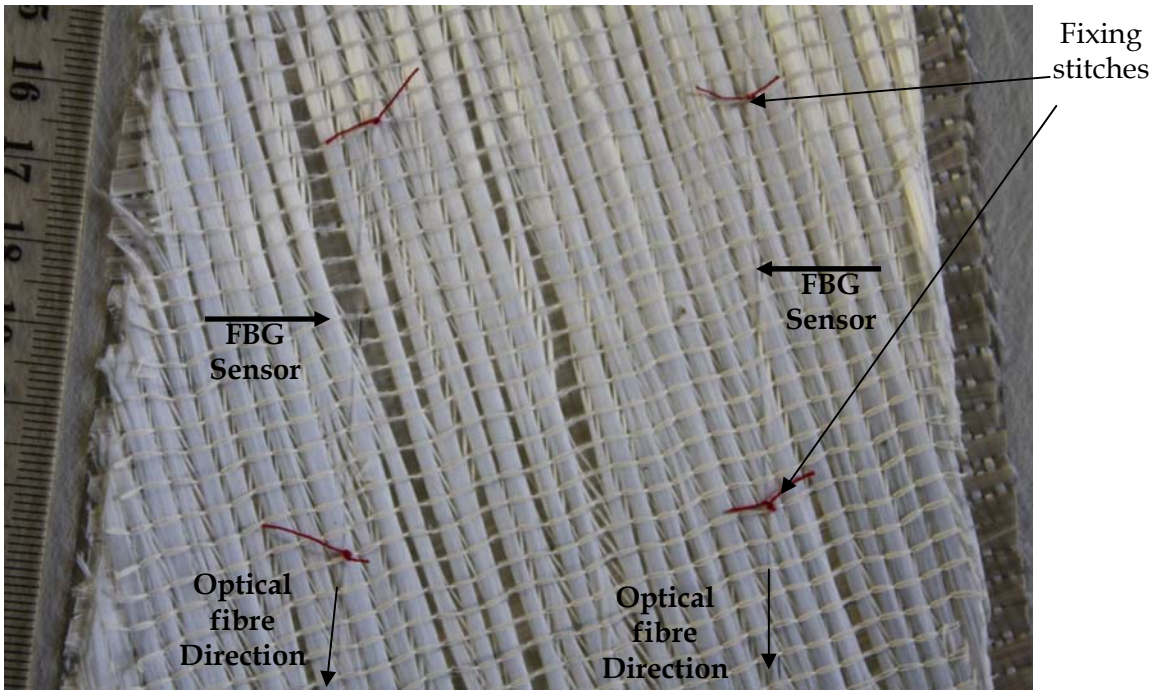

Figure 3: Close-up showing FBG sensor location and stitches to the woven glass ply on either side

The bottom side of the foil had one sensor array comprising 4 FBGs in 50 mm intervals running along the centre line of the foil and one array comprising 6 FBGs in 50 mm intervals running parallel to the trailing edge approximately 20 mm from the edge line as shown in foil view (a) in Figure 4.

The top side of the foil had one sensor array comprising 6 FBGs in 50 mm intervals stitched running parallel to the leading edge approximately 20 mm from the edge and one array comprising 4 FBGs in 50 mm intervals running parallel to the trailing edge approximately 20 mm from the edge as shown foil view (b) in Figure 4.

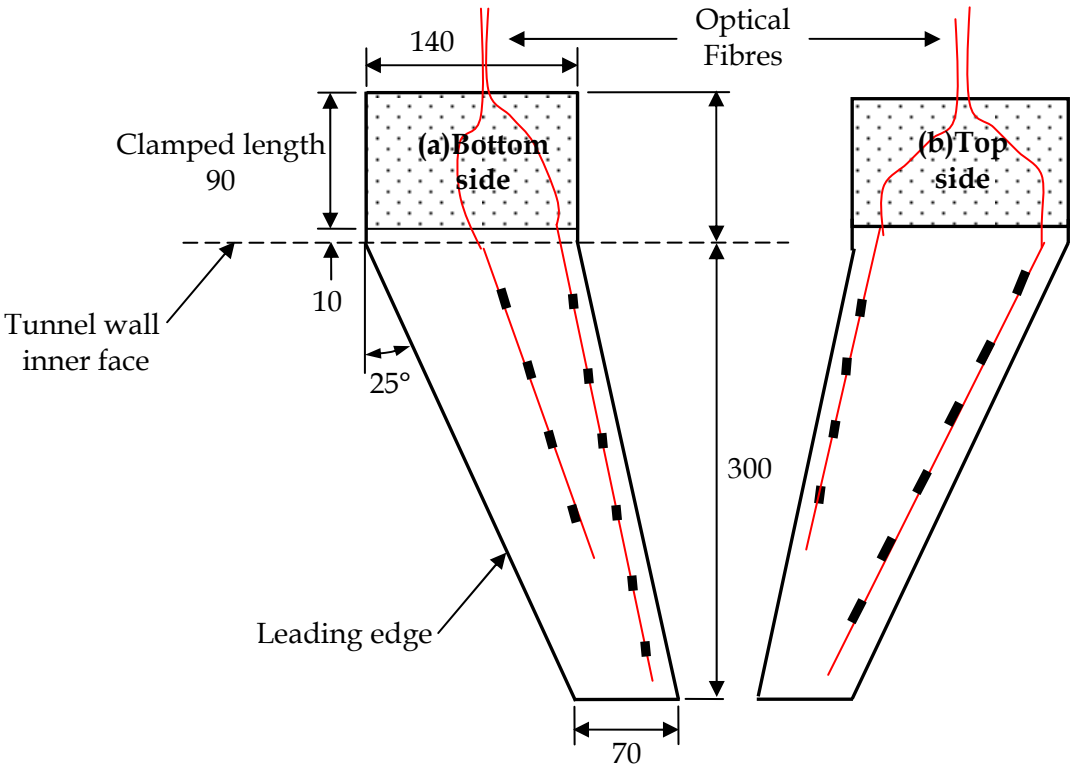

Figure 4: Schematic diagram showing foil dimensions and approximate sensor locations on the top and bottom sides of the foil. (All dimensions in mm)

The egress points of the fibre from the mould were sheathed in 3 mm (inner diameter) stainless steel tubing for protection with strain relief provided by Versalink® epoxy resin at the exposed tip of the steel tube. The base of the tube which was embedded in the foil was sealed with epoxy prior to infusion to prevent resin run-out along the interior of the tube. A photograph of the completed foil with embedded optical fibres is shown in Figure 5.

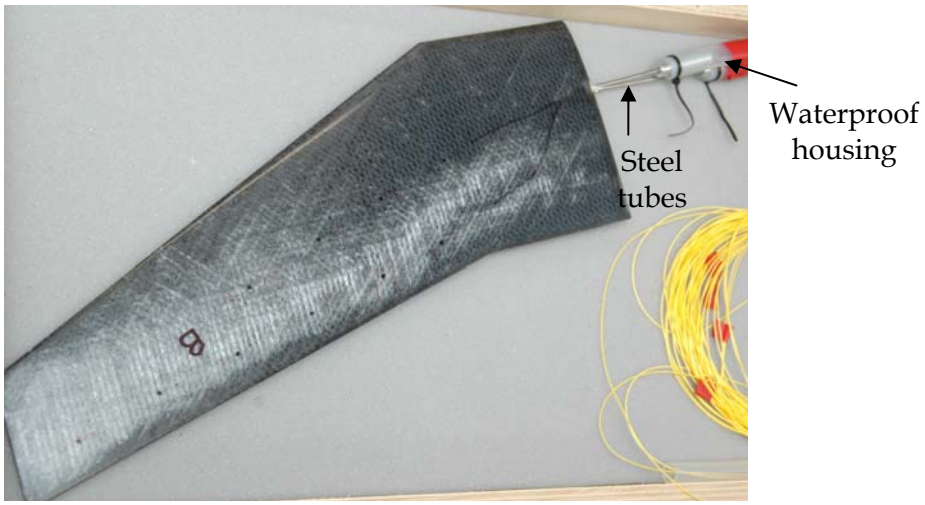

Figure 5: Photograph of infused foil showing steel tubes sheathing egress points of optical fibre and waterproof housing for cavitation tunnel tests

3. Foil Infusion Monitoring

An outline of the main features in the foil infusion sequence is shown in the table below:

Table 1: Sequence of events in foil infusion process

Stage	Elapsed Time(mins)	Event
1	0	Mould Placed in oven and allowed to equilibrate to 30 °C overnight
2	1100	Infusion Preparation commenced (oven temperature increased by 3 °C to compensate for opening of oven door
3	1160	Resin Infusion commenced
4	1330	Cleaning of resin run-out surrounding optical fibres (oven door open)
5	1360	Oven temperature increased to 40 °C
6	1490	Oven temperature increased to 50 °C and allowed to equilibrate overnight
7	2450	Oven switched off and mould allowed to cool
8	2650	Mould opened

The response data from each FBG array during the entire foil infusion process is shown in Figures 6 to 9. In these figures, the sensors in each fibre are numbered in ascending order from the root of the foil to the tip.

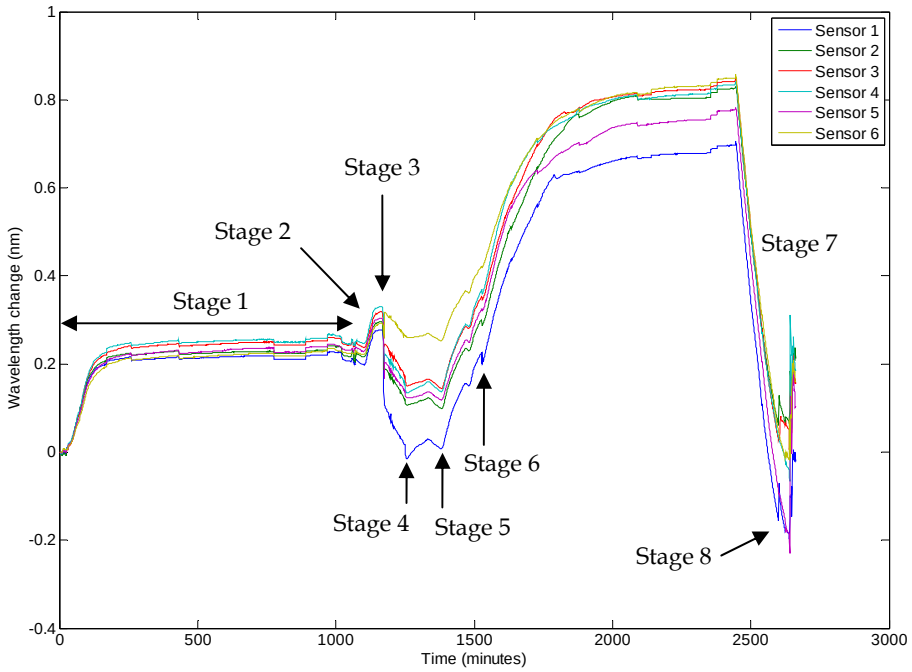

Figure 6: Response of FBG array located on the bottom side of the foil along the trailing edge during foil infusion and cure process

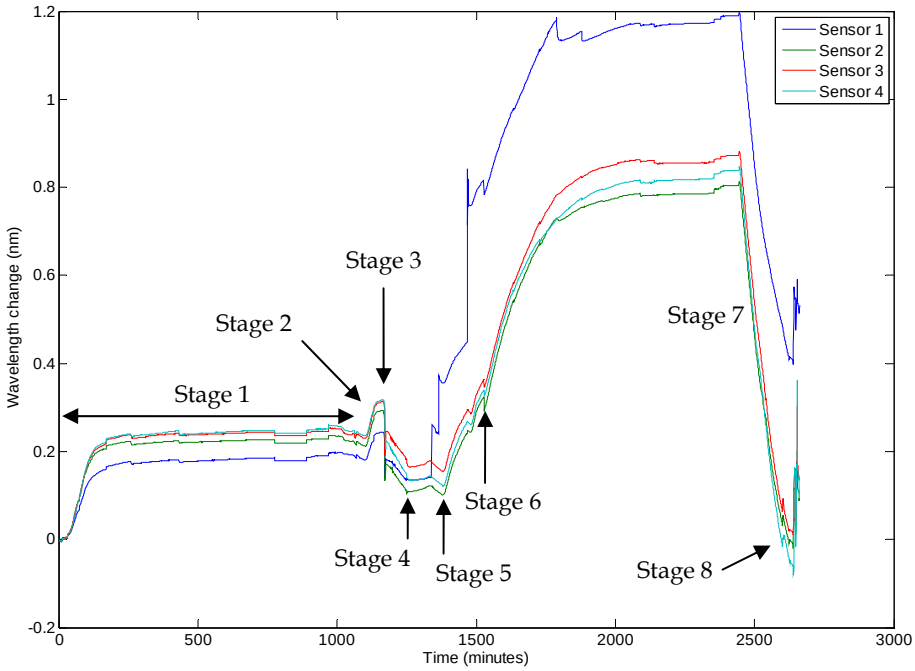

Figure 7: Response of FBG array located on the bottom side of the foil along the centre line during foil infusion and cure process

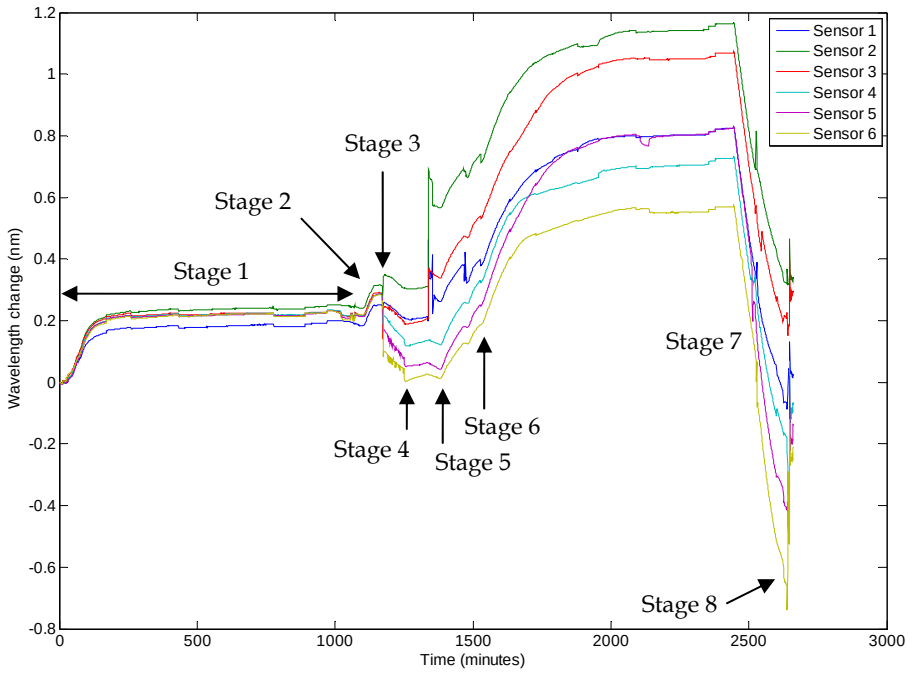

Figure 8: Response of FBG array located on the top side of the foil along the leading edge during foil infusion and cure process

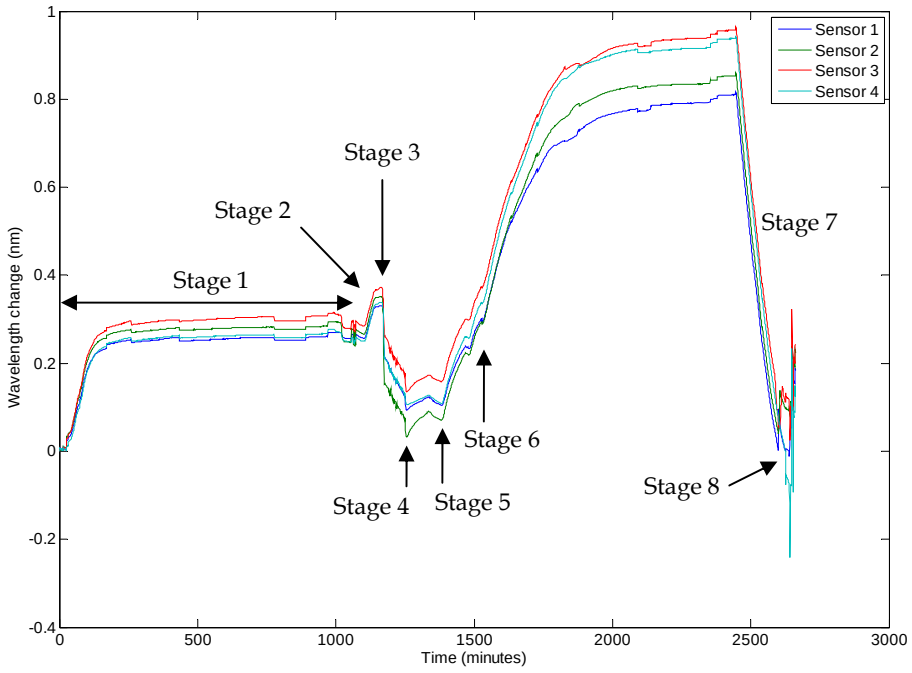

Figure 9: Response of FBG array located on the top side of the foil along the trailing edge during foil infusion and cure process

4. Cavitation Tunnel Tests

During the installation of the waterproof sheathing around the optical fibres and mating adaptors, one of the fibres (centre line of the bottom side of the foil) broke at the fibre to connector attachment. This occurred due to the limited clearance between the fibre connectors and the inner wall of the tube which made it difficult to feed the tubing over optical cables easily. Measurements were taken from the remaining three FBG arrays.

4.1 Variation of Angle of Attack (AoA)

The first set of tests looked at the response of the FBGs embedded in the foil to different angles of attack. Three sets of tests were conducted at the following conditions:

(1) Variation in AoA from +15 degrees to - 15 degrees (Reynolds No. (Re)= 0.5)
(2) Variation in AoA from +15 degrees to - 15 degrees (Reynolds No. (Re)= 1.0)
(3) Variation in AoA from +6 degrees to - 6 degrees (Reynolds No. (Re)= 1.5)

The AoA was changed in 0.5 degree increments dwelling at each angle for 8 seconds. As before the sensors in each fibre line are numbered in ascending order from the root of the foil to the tip. The response data from each FBG array is plotted in Figures 10 to 18.

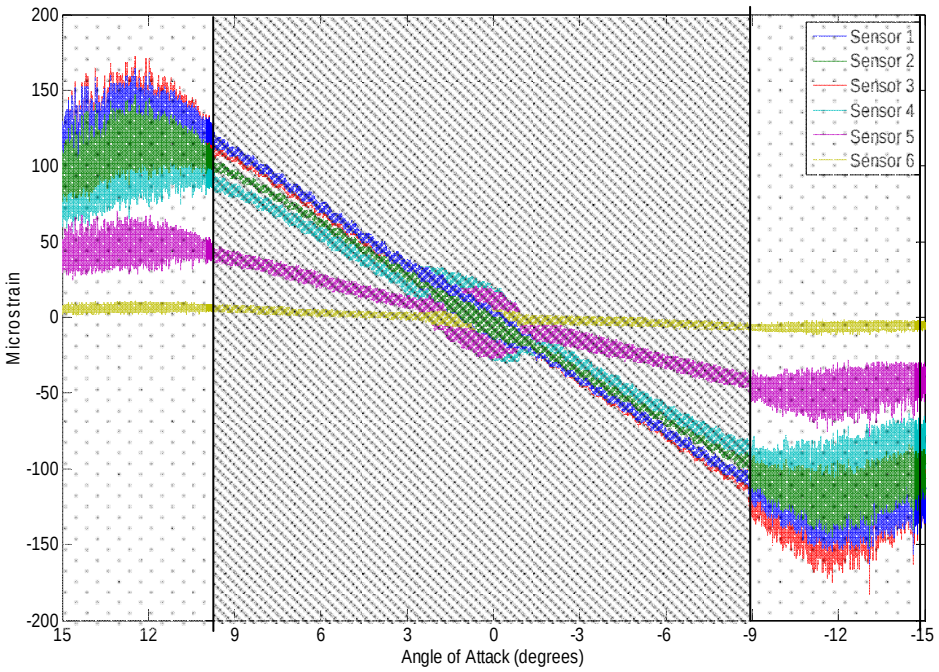

Figure 10: Strain response of FBGs for incremental increases in foil AoA from +15° to - 15° for trailing edge of bottom side of foil. (Re = 0.5)

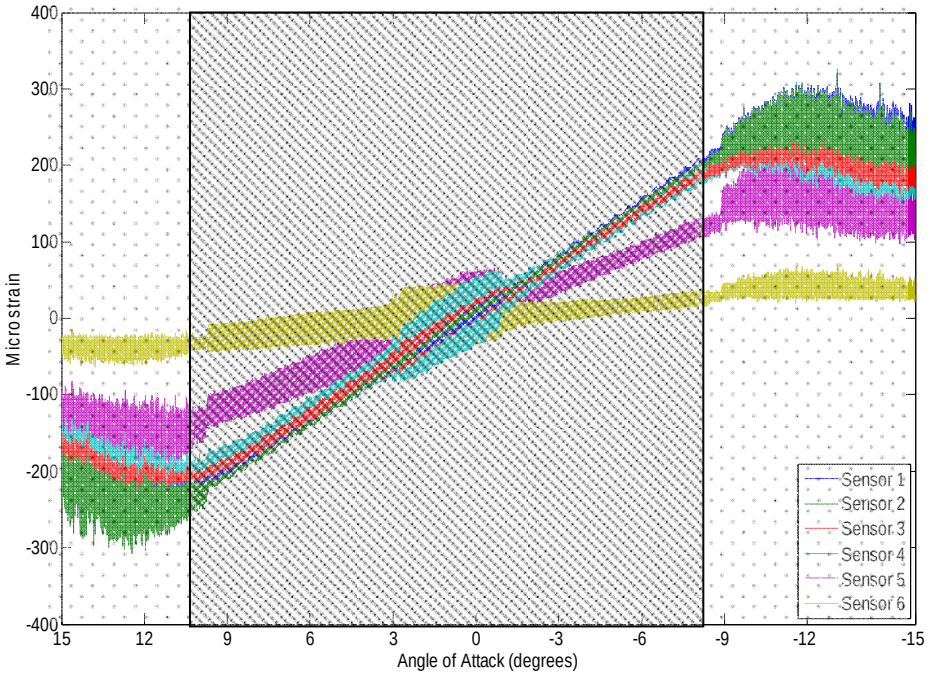

Figure 11: Strain response of FBGs for incremental increases in foil AoA from +15° to - 15° for leading edge of top side of foil. (Re = 0.5)

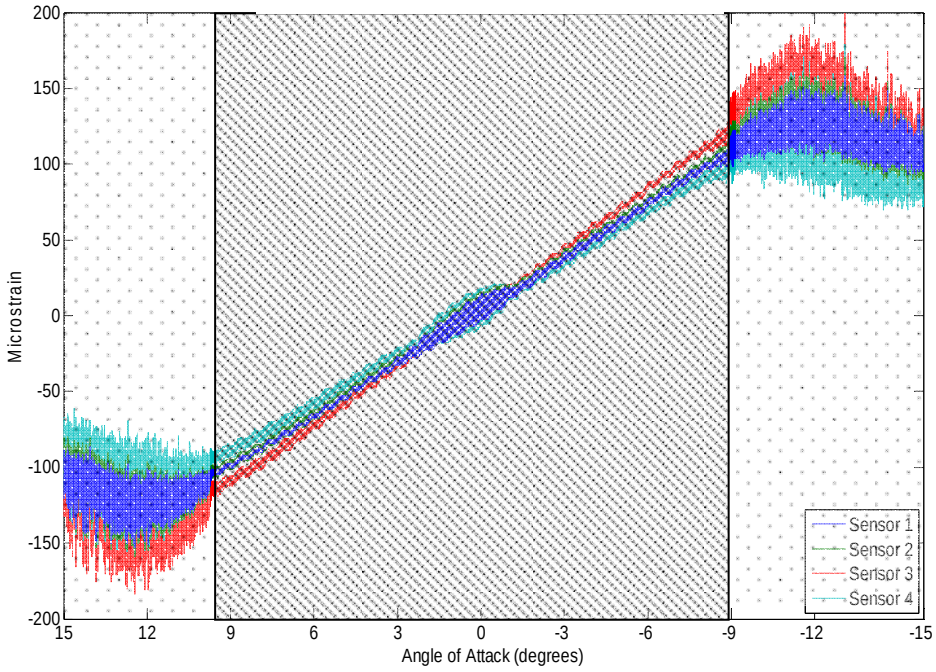

Figure 12: Strain response of FBGs for incremental increases in foil AoA from +15° to - 15° for trailing edge of top side of foil. (Re = 0.5)

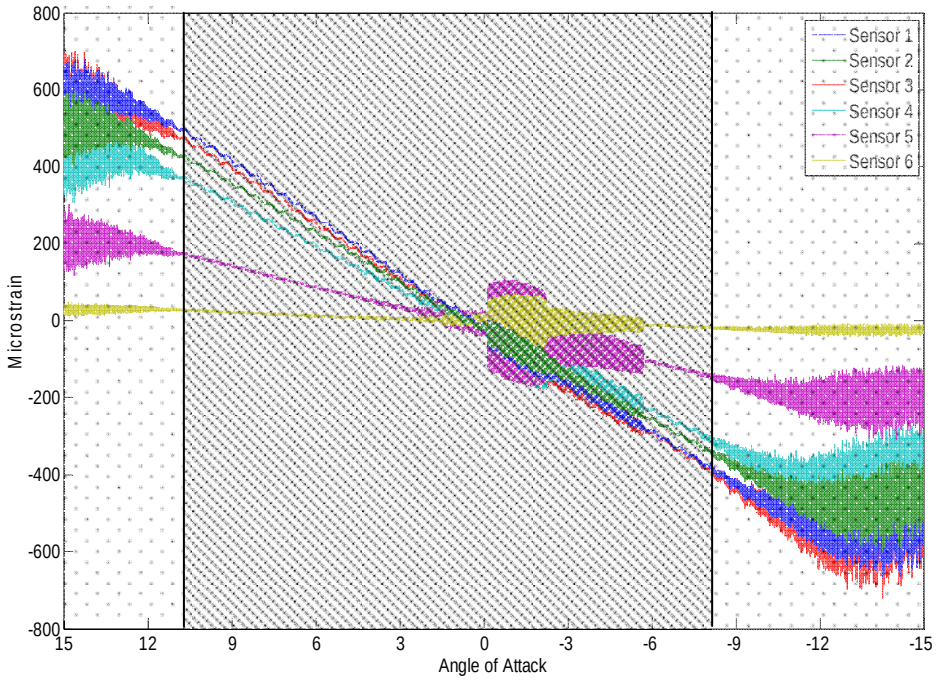

Figure 13: Strain response of FBGs for incremental increases in foil AoA from +15° to - 15° for trailing edge of bottom side of foil. (Re = 1.0)

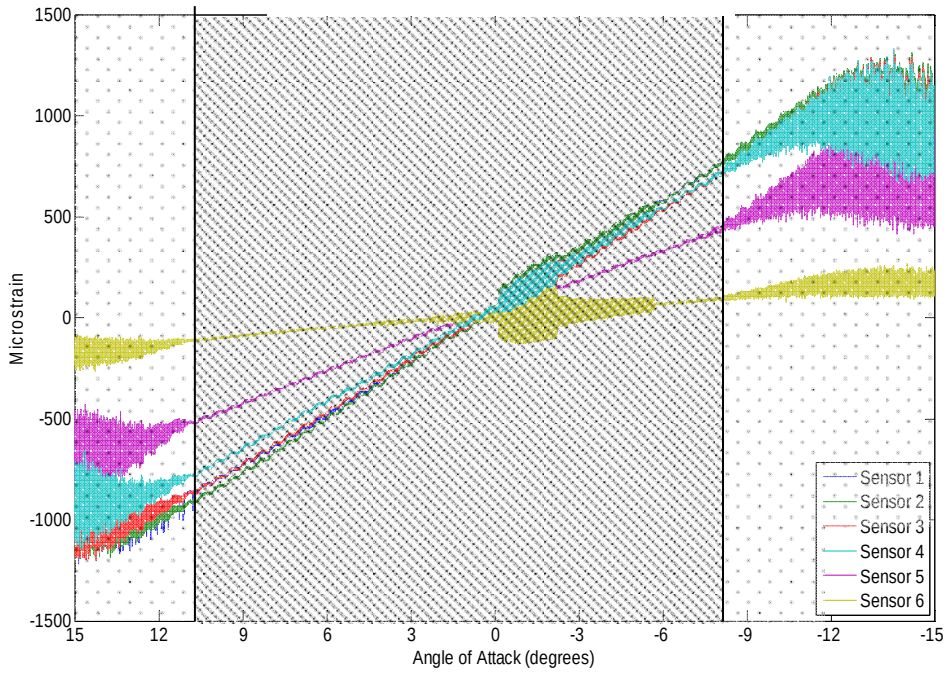

Figure 14: Strain response of FBGs for incremental increases in foil AoA from +15° to - 15° for leading edge of top side of foil. (Re = 1.0)

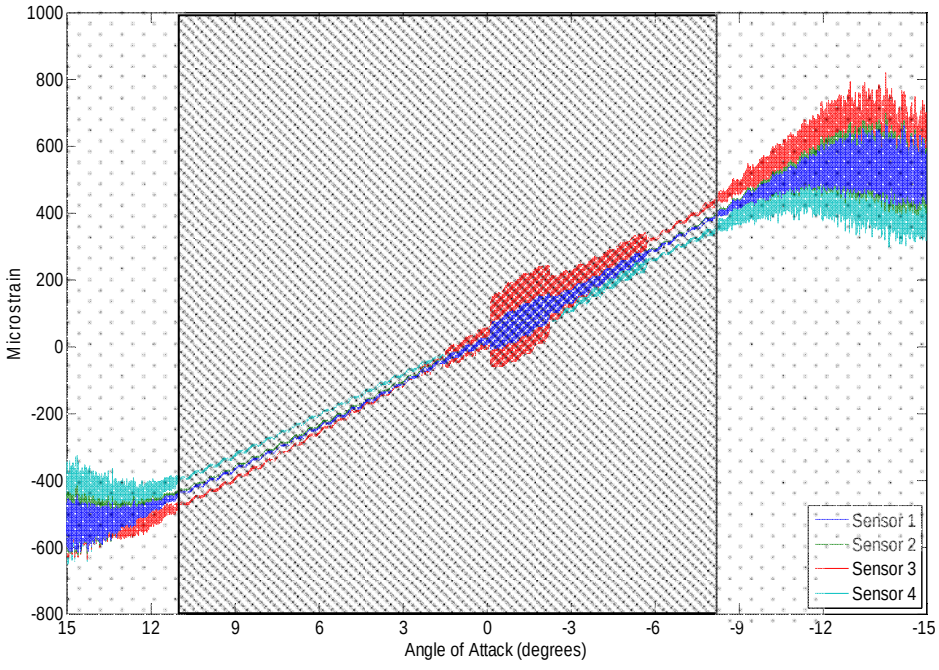

Figure 15: Strain response of FBGs for incremental increases in foil AoA from +15° to -15° for trailing edge of top side of foil. (Re = 1.0)

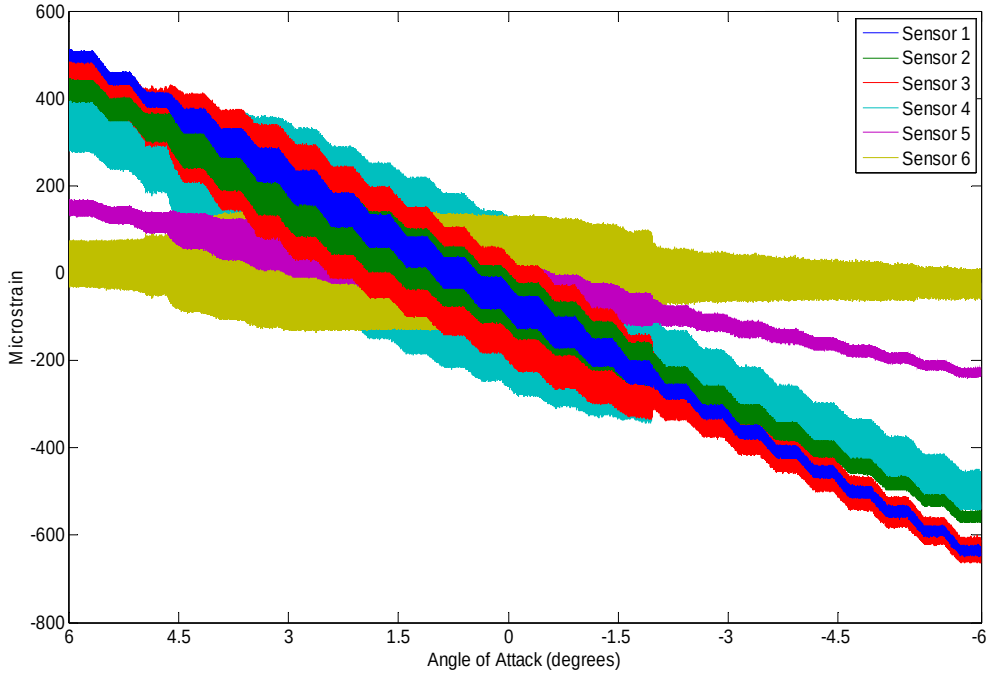

Figure 16: Strain response of FBGs for incremental increases in foil AoA from +6° to - 6° for trailing edge of bottom side of foil (Re = 1.5)

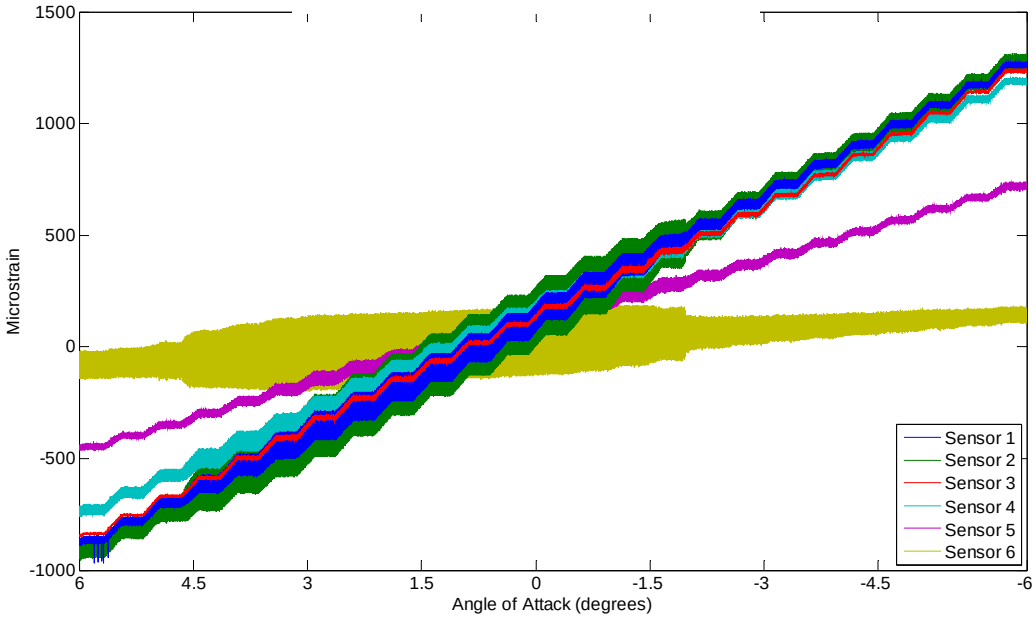

Figure 17: Strain response of FBGs for incremental increases in foil AoA from +6° to - 6° for leading edge of top side of foil (Re = 1.5)

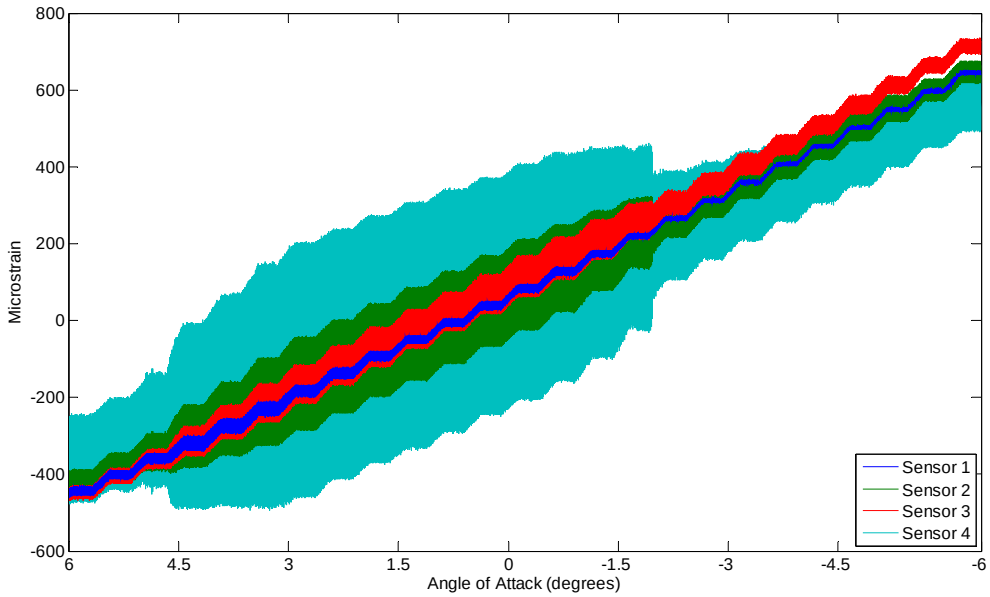

Figure 18: Strain response of FBGs for incremental increases in foil AoA from +6° to - 6° for trailing edge of top side of foil (Re = 1.5)

4.2 Variation of Cavitation Tunnel Pressure

For the next set of tests, the foil was fixed at zero degrees AoA with no water flow (Reynolds No. = 0) while the cavitation tunnel pressure was decreased from 150 kPa to 50 kPa in 10 kPa steps with a 30 second dwell time at each pressure step. This data is plotted in Figures 19 to 21.

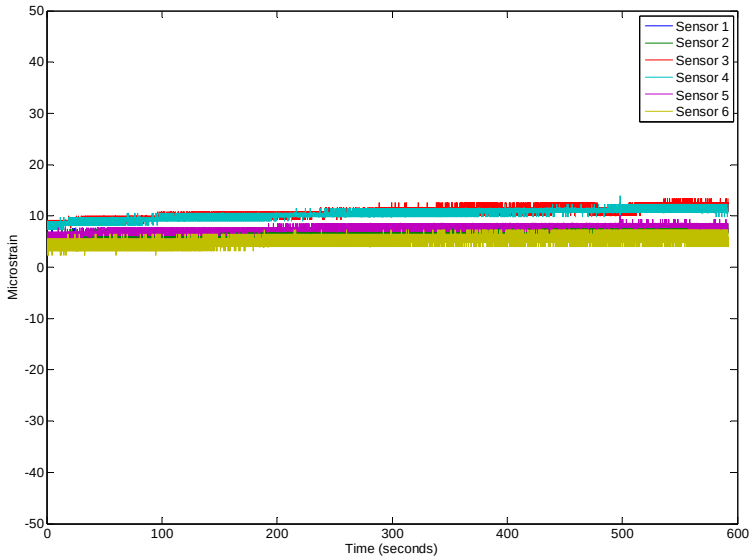

Figure 19: Time response of FBGs for incremental decreases in tunnel pressure from 150 – 50 kPa for trailing edge of bottom side of foil (Re = 0)

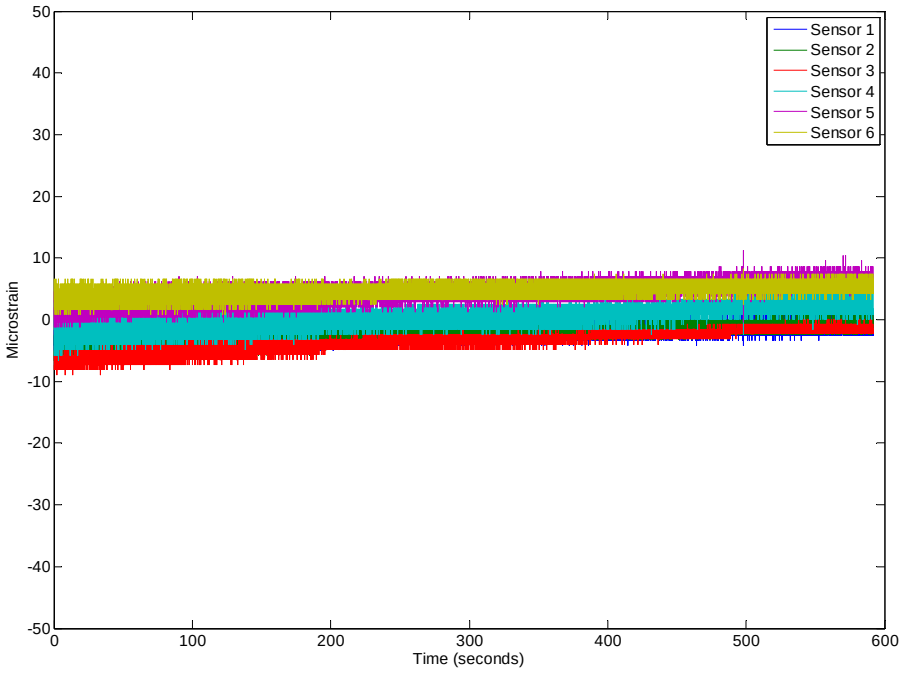

Figure 20: Time response of FBGs for incremental decreases in tunnel pressure from 150 – 50 kPa for leading edge of top side of foil (Re = 0)

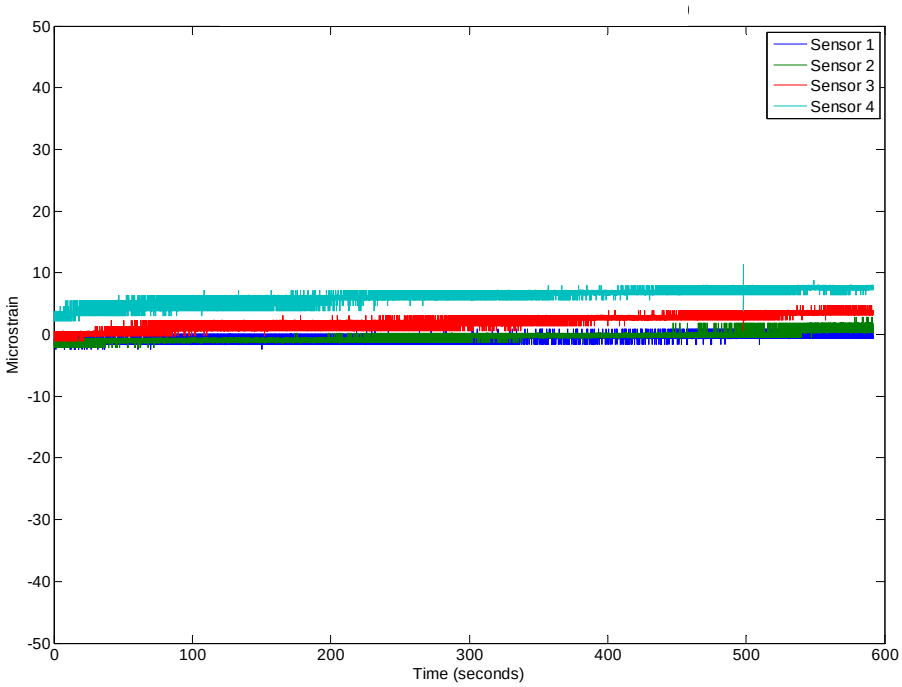

Figure 21: Time response of FBGs for incremental decreases in tunnel pressure from 150 – 50 kPa for trailing edge of top side of foil (Re = 0)

5. Analysis

5.1 Variation in AoA (+15° to –15°) @ Reynolds No. = 0.5

For a Reynolds number of 0.5, there appears to be two distinct flow regimes dependent on the AoA of the foil. For most of the angular range of the foil (+10° to -9°) the strains measured by the FBGs in the foil have two components: a static strain level which is linearly dependent on the AoA and a periodic sinusoidal variation in strain which varies slightly in frequency as a function of the AoA as represented schematically in Figure 22 and shown numerically in Figure 23. This periodic vibration increases in magnitude at an AoA approaching 0° and was confirmed visually in the cavitation tunnel. However, at the time of testing there was no instrumentation in place to measure the tip deflection independently so it was not possible to correlate the frequency of the observed vibration with those measured in the foil by the FBGs.

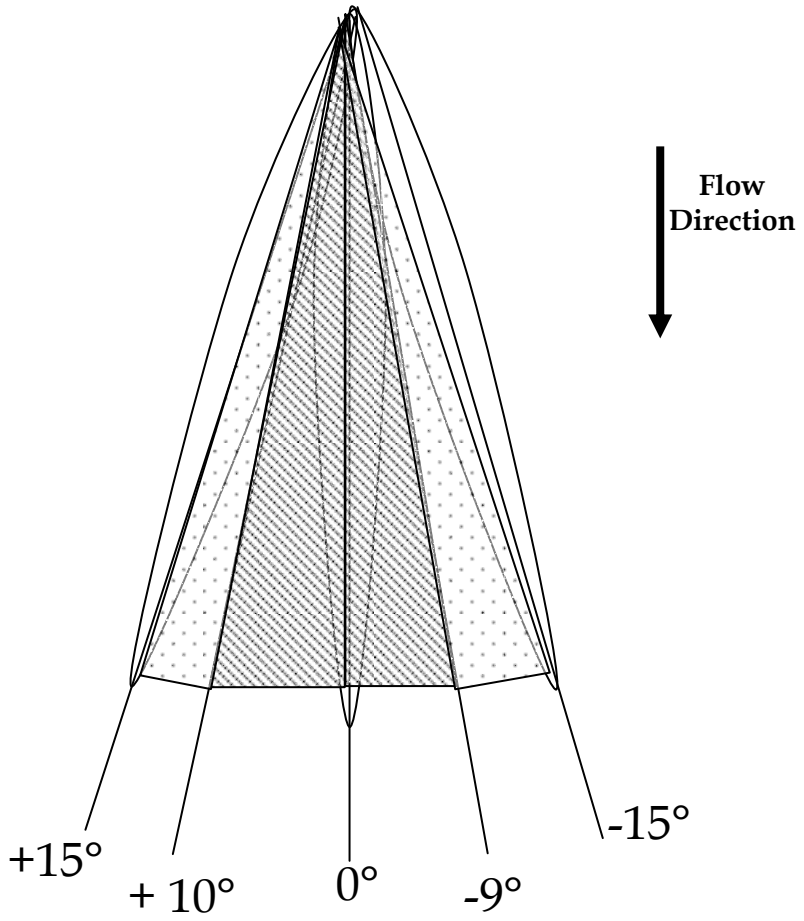

Figure 22: Two different flow regimes for different foil angles at Re=0.5. Shadings within foil angles correlate to boundaries of response regions indicated in Figures 10 to 12.

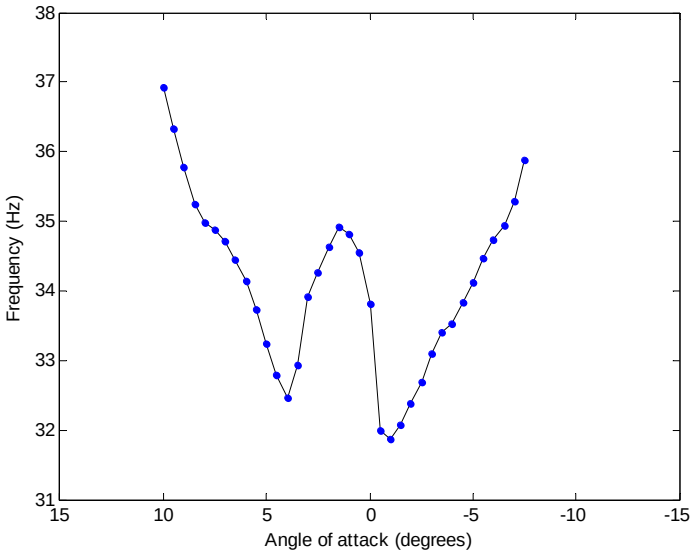

Figure 23: Resonant frequency of strain response data from single FBG as a function of foil AoA for Re=0.5 (Note: the response was the same for all FBGs)

At a relatively steep foil angle of attack (-9° < AoA > +10°), the FBG response becomes more random in nature as indicated by the power spectral density plot in Figure 24, suggesting a turbulent flow regime possibly due to flow separation. There is a 1 degree asymmetry in the onset of this random response on either side of the zero axis.

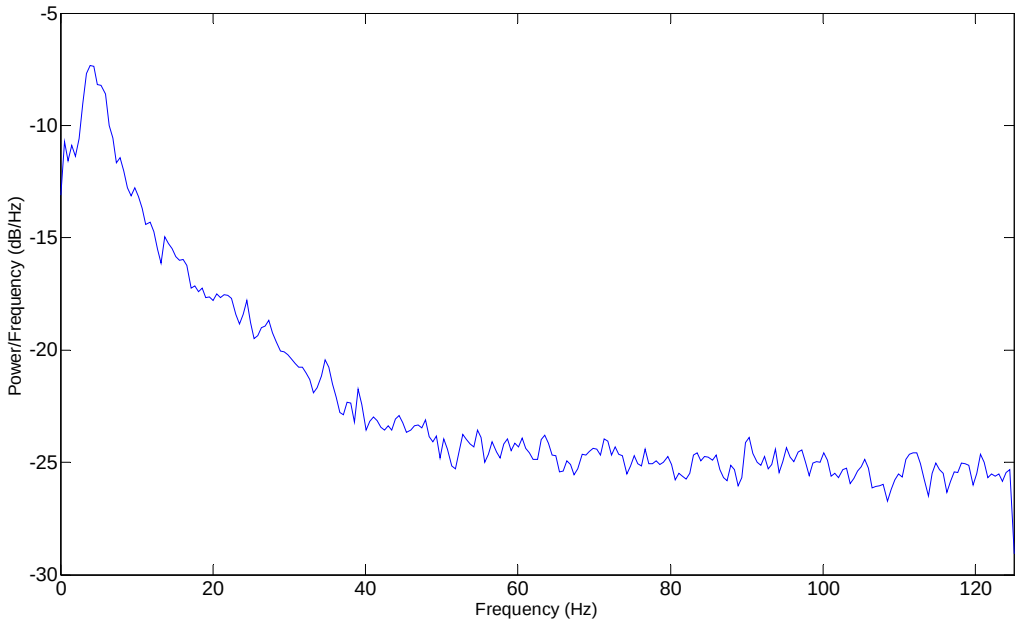

Figure 24: Power spectrum of response data from single FBG at 15° AoA for Re = 0.5

For both flow regimes the strain levels along the foil increase towards the root as expected.

5.2 Variation in AoA (+15° to –15°) @ Reynolds No. = 1.0

For measurements taken at Re = 1.0 there are again two different flow regimes dependent on the AoA of the foil.

For most of the angular range of the foil (11° to -8°) the strains measured by the FBGs show a static strain level which is dependent on the angle of the foil. The overall strain levels were also higher than those measured at Re = 0.5 which was expected. However, at this Re the sinusoidal component of the strain response is only seen at the negative AoA up to 5°. This response was similar in its asymmetry for all three FBG arrays on both surfaces of the foil but this asymmetry was slightly larger than for Re = 0.5. As before, the frequency of these sinusoidal variations varies slightly with the AoA as shown in Figure 25.

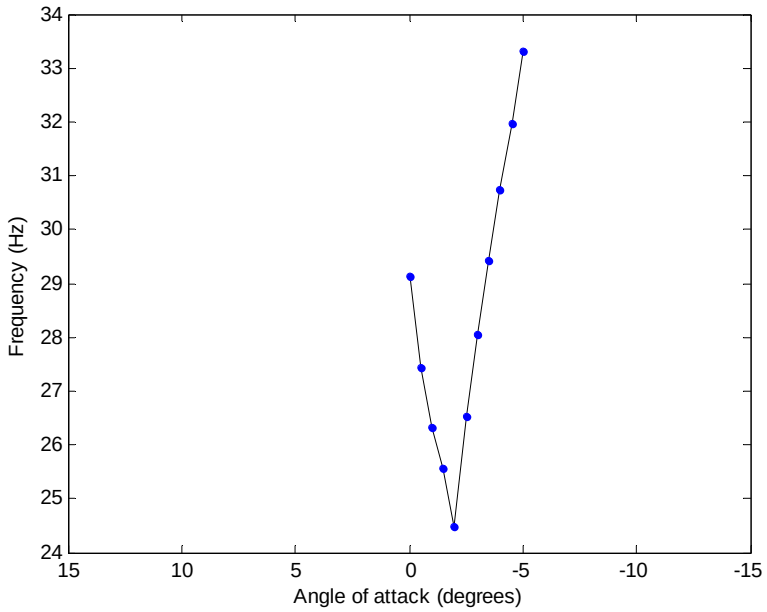

Figure 25: Resonant frequency of strain response data as a function of AoA for Re = 1.0

As observed in the previous section, for the lower Re, for a Re = 1.0 at a relatively steep AoA (-9° <AoA > +11°), the FBG response becomes more random in nature as indicated by the power spectral density plot in Figure 26. There is again a 2 degree asymmetry in the onset of random response on either side of the zero axis.

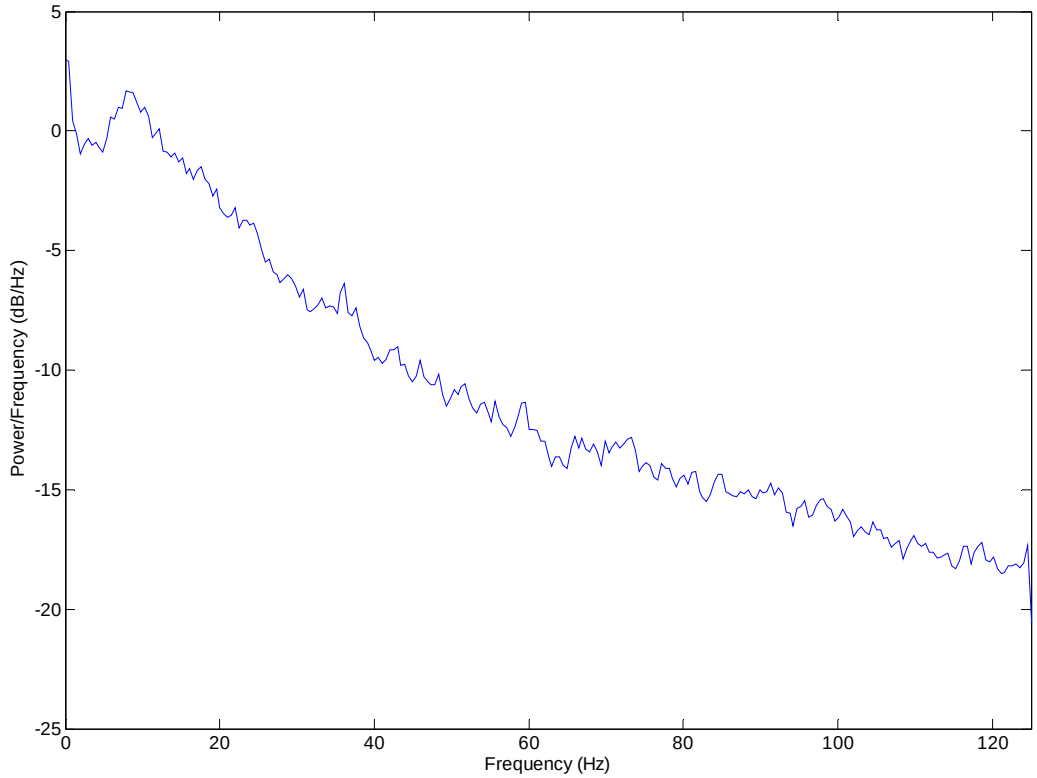

Figure 26: Power spectrum of response data from single FBG at 15° AoA at Re = 1.0

Again for both flow regimes the strain levels along the foil increase towards the root as expected.

5.3 Variation in AoA (+6° to –6°) @ Reynolds No. = 1.5

For the final experiment the range of angles through which the foil was rotated was reduced to +6° to - 6°. This was done to minimise the risk of damaging the foil at higher flow velocities. Within this reduced range no random vibrations were measured by the FBGs. The response of the FBGs had two components: a static strain level which was linearly dependent on the AoA of the foil and a periodic sinusoidal variation in strain which varied slightly in frequency with the AoA as shown in Figure 27.

A visual confirmation of the periodic deflections in the foil tip was not possible because of the high frequency of the oscillations. It should also be noted that the vibration frequencies are close to the Nyquist limit for the FBG interrogation system.

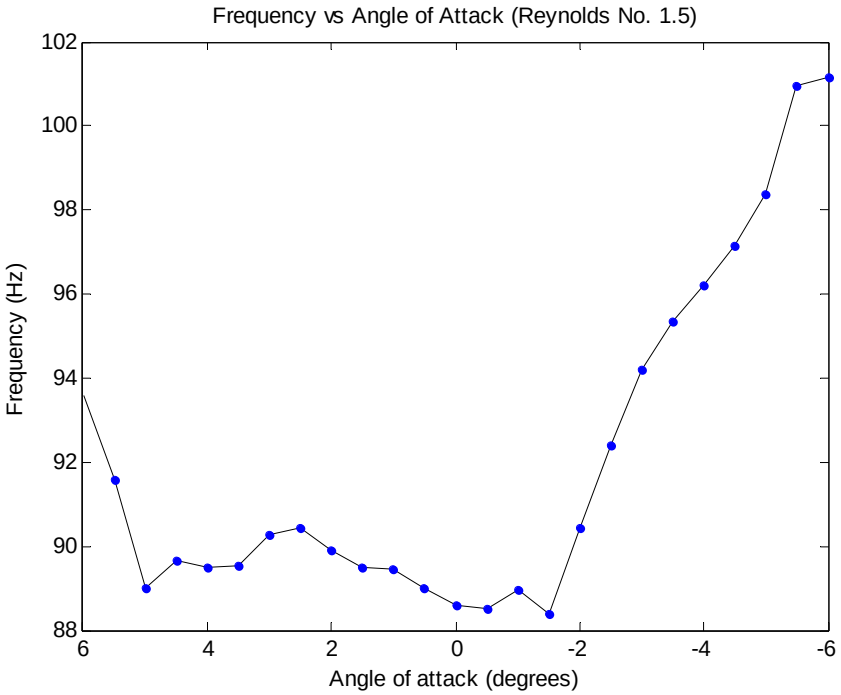

Figure 27: Resonant frequency of strain response data as a function of AoA for Re = 1.5

As for the previous two flow rates, the strain levels along the foil increase towards the root as expected. The overall strain levels were higher than those measured at a Reynolds number of 0.5 and 1.0 which was also expected.

5.4 Variation of Cavitation Tunnel Pressure

The measured response from the FBGs shown in Figures 19 to 21 clearly show that there is no significant response to hydrostatic tunnel pressure for the pressure range from 50 to 150 kPa. There is a small drift upwards over the 600 second time internal which may be due to temperature variation. The drift in wavelength is approximately 3pm which would be equivalent to 0.3 °C increase over 10 minutes.

6. Conclusions

The results clearly demonstrate that FBG arrays embedded in a shape adaptive composite foil are able to measure surface strain under different hydrodynamic loading conditions. The sensors are able to detect whether the foil is oscillating at a fixed frequency, vibrating in a random manner or experiencing a static deflection. The strain gradient from root to tip can also be measured under different loading scenarios. There does not appear to be any significant sensitivity of the FBGs to hydrostatic pressure in the pressure range from 50 to 150 kPa.

7. Future Work

This program of work revealed several issues that need to be addressed in order to effectively use distributed FBG arrays to measure deflected shape and inter-laminar strains.

Firstly the FBG strain data needs to be converted to a deflection shape measurement. This will involve consideration of both the rigid body rotation and simple beam deflection theory using a finite difference method to calculate the deflections. The calculated deflection shapes can then be independently validated by simultaneous independent measurements of foil deflection using a scanning laser vibrometer. This data will be used to verify, and if necessary refine, the finite element model of the foil. It is anticipated that the initial validation work for the conversion of strain data to deflection shape will require the manufacture of a simpler non-twisted foil design with a higher density of embedded FBG sensors.

The FBG sensors used in these preliminary trials were embedded just below the top and bottom surface of the foil. In order to measure inter laminar strains in the foil, FBG arrays will be required to be embedded between woven composite plies deeper within the foil lay-up. There is potential for this to cause resin rich areas surrounding the optical fibre. Furthermore, the reinforcing fibres may apply transverse strains on the optical fibre, inducing strain gradients which would result in a non-linear FBG response to strain. Further experimental work is required to determine whether these are significant issues and if so, to develop corrective actions to minimise the effects.

The cross-sensitivity to pressure was only measured over a limited pressure range due to concerns over water leaks at the optical fibre egress point at higher tunnel pressures. In order to fully characterise the response of the FBGs to pressure, it is recommended that the foil be tested in a pressure vessel over an extended pressure range.

Finally, there are also several engineering challenges remaining, mainly associated with the egress point of the optical fibres from the composite part and the incorporation of the data transmission fibre within the force balance unit of the foil mounting assembly in the tunnel.

8. Acknowledgements

The authors gratefully acknowledge the assistance of the following people during the course of this work; Dr Brendon Anderson for program support, Dr. Nigel St John (DSTO) and Mr. Russell Cairns (DSTO) for fabrication of the composite foil, Assoc. Prof. Paul Brandner (AMC), Dr. David Clarke (DSTO) and Mr Bryce Pearce (AMC) for assistance with the cavitation tunnel experiments. The authors also acknowledge the Office of Naval Research for the support of this work under the Naval International Cooperative Opportunities in Science and Technology Program.

DEFENCE SCIENCE AND TECHNOLOGY ORGANISATION
DOCUMENT CONTROL DATA

1. PRIVACY MARKING/CAVEAT (OF DOCUMENT)

2. TITLE

Initial Trial using Embedded Fibre Bragg Gratings for Distributed Strain Monitoring in a Shape Adaptive Composite Foil

3. SECURITY CLASSIFICATION (FOR UNCLASSIFIED REPORTS THAT ARE LIMITED RELEASE USE (L) NEXT TO DOCUMENT CLASSIFICATION)

Document	(U)
Title	(U)
Abstract	(U)

4. AUTHOR(S)

Claire Davis, Patrick Norman, James Kopczyk and David Rowlands

5. CORPORATE AUTHOR

DSTO Defence Science and Technology Organisation
506 Lorimer St
Fishermans Bend Victoria 3207 Australia

6a. DSTO NUMBER	6b. AR NUMBER	6c. TYPE OF REPORT	7. DOCUMENT DATE
DSTO-TN-1070	AR-015-236	Technical Report	February 2012

8. FILE NUMBER	9. TASK NUMBER	10. TASK SPONSOR	11. NO. OF PAGES	12. NO. OF REFERENCES
2012/1014115/1	CERP 07/292	CDS	19	-

13. DSTO Publications Repository

http://dspace.dsto.defence.gov.au/dspace/

14. RELEASE AUTHORITY

Chief, Air Vehicles Division

15. SECONDARY RELEASE STATEMENT OF THIS DOCUMENT

Approved for public release

OVERSEAS ENQUIRIES OUTSIDE STATED LIMITATIONS SHOULD BE REFERRED THROUGH DOCUMENT EXCHANGE, PO BOX 1500, EDINBURGH, SA 5111

16. DELIBERATE ANNOUNCEMENT

No Limitations

17. CITATION IN OTHER DOCUMENTS Yes

18. DSTO RESEARCH LIBRARY THESAURUS

Bragg Gratings, deflection shape, shape adaptive, composites

19. ABSTRACT

This technical note reports on the embedment and testing of a series of distributed optical fibre sensors embedded just beneath the top and bottom surfaces of a shape adapative composite foil. The sensors were monitored during the resin infusion and curing stages of the composite foil fabrication process. The cured foil was tested in a variable pressure water tunnel at different flow rates, angles of attack and tunnel pressures to characterise the distributed strain response of the foil to these parameters.